SUBSONIC AERODYNAMIC PREDICTION OF SHUTTLE-LIKE CONFIGURATIONS USING NONLINEAR VORTEX-LATTICE METHOD

ICAS-88-4.4.2

D. Almosnino* and J. Rom**
Technion - Israel Institute of Technology
Haifa 32000, Israel.

Abstract

A nonlinear vortex-lattice method for arbitrary cross-section bodies in subsonic flow is applied to predict the aerodynamic characteristics of shuttle-like configurations based on NASA orbital vehicle. The effect of vortex separation at medium/high angles of attack is calculated and discussed. Computed results include aerodynamic coefficients, pressure distributions and also local effects due to geometry modifications. The results are generally in good agreement with wind-tunnel and flight test data. It is concluded that the method can be used for preliminary design and analysis purposes of complex body geometries such as the space shuttle.

List of Symbols

C_D - drag coefficient
C_L - lift coefficient
C_{L0} - lift coefficient at $\alpha=0$
$C_{L\alpha}$ - lift coefficient vs. α curve slope
C_m - pitching moment coefficient
C_{m0} - pitching moment coefficient at $\alpha=0$
$C_{m\alpha}$ - pitching moment coefficient vs. α curve slope
$C_{N\alpha}$ - normal force coefficient vs. α curve slope
C_p - pressure coefficient
M - Mach number
x_{cp} - center of pressure (measured from nose tip
α - angle of attack
δ_{BF} - body flap deflection angle
δ_e - wing elevons deflection angle

Reference Dimensions (all in inches unless otherwise noted):

C_{ref} - mean aerodynamic chord (474.81)
L_B - reference body length (1290.3)
S_{ref} - reference wing area (2690 ft^2)
b - wing span (938.68)
X_{ref} - axial location of moment reference point ($0.65L_B$)
Z_{ref} - height of moment reference point above body axis (37.2)

Introduction

Space shuttle configurations are designed to fly through a very wide range of flow regimes. Most of the atmospheric flight of the shuttle vehicle takes place at hypersonic or supersonic Mach numbers. However, one of the most critical parts of their flight, namely the final approach and landing, takes place at subsonic Mach numbers and at high angles of attack. The aerodynamics of the landing flight is dominated by the effects of vortex separation, emanating from the wing leading-edges and sometimes from the fuselage as well. The separated vortex flow rolls up over the wing surface and causes a nonlinear addition to the lift coefficient as the angle of attack increases. The vortex wake may affect control surfaces as well. Accurate prediction of the aerodynamic coefficients in this flow regime is important due to the small margin of error permitted at this stage of flight. High rate of energy losses with no possibility of "go around" are some of the main limitations that need to be considered in the aerodynamic design process of the space shuttle configuration for the subsonic landing flight. It is therefore necessary to have design and analysis tools that can predict the aerodynamic characteristics of shuttle-like flight vehicles in subsonic flow, as much as in the other flow regimes.

The aerodynamic design considerations and the development steps of NASA space shuttles have been extensively documented since the beginning of the space shuttle project (e.g. Refs. 1-4). The aerodynamic data base obtained for these space shuttles is very useful for the purpose of comparison with analytical results and verification of the accuracy of new analyses as design tools. The actual development of NASA space shuttles is based heavily on thousands of wind-tunnel test-hours, due in part to the limited capacity of computers and computational methods available at the beginning of that project. The state of the art of computers and computational methods at present can save some of the design expenses involved in wind-tunnel testing. In particular, the elimination process between preliminary proposed configurations and the assessment of the

* Research Fellow, Faculty of Aeronautical Engineering, Member AIAA.

** Lady Davis Professor, Faculty of Aeronautical Engineering, Fellow AIAA.

Copyright © 1988 by ICAS and AIAA. All rights reserved.

possible effects of various modifications on the desired configuration are just two examples where computational methods should take an important part.

In the present work, a nonlinear vortex lattice method for the calculation of the aerodynamics of arbitrary cross-section bodies in subsonic flow[5] is utilized to compute the characteristics of models that are geometrically similar to the NASA space shuttle.

Method of Calculation

The present calculations are performed using the Non-Linear Vortex Lattice Method for arbitrary cross-section bodies[5]. The present method is a modification and extension of the axisymmetric body computer code[6-7]. The modification consists of replacing the point source distribution along the body axis with a surface source panel distribution, describing the thickness effect of the body at zero angle of attack. The input options are extended to accept general shapes of bodies with various cross-sections.

The computation process is described schematically in the flow chart of Fig. 1. The calculation process starts with the definitions of the cross-sections of the body and the division of the body into elemental panels, then proceeds to the calculation of the source panel distributions that describe the thickness effect of the body at zero angle of attack. The body is then placed at a desired angle of attack, at which the corresponding bound vortex distribution is calculated. So, the calculated flow field includes the effect of incidence while taking into account the velocity induced by the previously calculated source distribution. The solution itself is obtained by fulfilling the boundary condition of zero normal velocity at the predetermined control points on the surface of the body in each panel. Vortex separation points along the body are usually predefined by the user from empirical considerations. In the first sweep, an initial position of the vortex lines that represent the vortex wake is assumed (see also Ref. 7). After the bound vortices strength is first calculated, the strengths of the free vortices are computed. The free vortices are then aligned with the local flow direction to fulfill the free surface boundary condition for the wake (this process is described in more detail in Ref. 7). The change that occurs in the geometry of the wake demands a new iteration to compute the corresponding new bound vortex distribution. This iterative process continues until full convergence of the free vortices path and bound vortices strength is achieved. Finally, the surface pressure distribu- and the aerodynamic coefficients are computed using the converged solutions of the vortex and source-panel systems calculated for the vehicle configuration at that fixed angle of attack.

The input of the nonlinear vortex-lattice method includes user definition of the vortices separation points along the body. When a wing has a sharp leading-edge, the definition of these points is obvious. In the present case the shuttle wing has a rounded leading-edge, which is thick at the apex of the wing and becomes relatively sharp as the local span grows towards the base of the configuration. Having very little details on the actual separation line, the separation points in the present study are selected to be close to the leading-edge apex, starting from slightly inner position at the blunt apex of the wing and gradually reaching the leading-edge apex as the edge becomes sharper. The final position of the separation points used in the present study is the result of careful analysis of the pressure distribution and some trial and error process in a few preliminary runs of the computer code.

Computer Model of the Shuttle Vehicle

The model used in the present calculations is based on an early NASA Orbiter Vehicle geometry designated "OV-89-B" (Ref. 8), with a double-delta leading-edge sweep of 79/45 degrees and a straight angle trailing-edge sweep. The full model includes canopy and OMS pods (Fig. 2), but does not have the vertical fin and no body flap. Calculations are performed also for models without canopy or OMS pods to analyze the aerodynamic effect of their presence. The wing elevon deflection is zero through all calculations.

Panelling of the model includes 26 panels along the vehicle axis and 27 panels over half the circumference of each cross-section (Fig. 3). The use of the present panelling scheme, that is originally intended for more slender configurations, causes some clustering of panels near the "wing line" in the nose section (Fig. 3), however, this fact is found to cause no problems to the numerical solution process. The computation involves a grid of 702 panels over half of the body (only longitudinal characteristics are included in the present study).

Results

The aerodynamic coefficients are calculated for angles of attack of up to 25 degrees. In most cases the flow can be considered incompressible. Comparison is made with experimental data obtained at low subsonic Mach numbers (Refs. 2-4

and 9-10), and also with some other computational methods (Ref. 11).

The lift coefficient variation with angle of attack is shown in Fig. 4. At small angles of attack the results of the present method for unseparated flow conditions almost coincide with the computed results of Ref. 11 for M=0.25. The calculated normal-force curve slope of $C_{N\alpha}$=0.052 1/deg is in excellent agreement with the flight-test data presented in Ref. 9. At zero incidence the present method as well as Ref. 11 present a slightly higher value for C_{L0} (-0.019) than the experimental one which is about -0.05 (Refs. 2-3). The reason for this difference is not clear, however, this can be attributed to the simplifications made in the geometrical description of the model, such as the absence of the body flap. At angles of attack above 12 degrees the present unseparated flow solution under-predicts the lift coefficient, while the separated vortex flow results fit the experimental data quite well (Fig. 4), showing that nonlinear increase of the lift coefficient does result from the added vortex lift.

The variation of the pitching moment coefficient as a function of the lift coefficient is presented in Fig. 5. At small incidence (at 5.73 deg angle of attack) the calculated value of $C_{m\alpha}$ is -0.0008. This value is in very good agreement with wind tunnel data (Ref. 3) and flight-test data (Ref. 9). As a result of the good prediction of $C_{m\alpha}$ and $C_{L\alpha}$, the calculated center of pressure location is also within the acceptable range of uncertainty cited in Ref. 3. The calculated value of x_{cp}/L_B is 0.68, while Ref. 3 cites a nominal value of 0.67 with an uncertainty range of ±0.015 at M=0.3. On the other hand, it is clear from Fig. 5 that there is a shift between the predicted value of C_{m0} - the pitching moment coefficient at zero lift (which is -0.015) and the experimental value (0.05) obtained at M=0.25 (Ref. 3). The reason for this discrepancy is not clear. It should be noted however that the absolute value of C_{m0} is small, almost zero, in both cases. The wind tunnel uncertainty correlation quoted in Ref. 3 is ±0.005 for low subsonic Mach numbers. The present calculated value of C_{m0} fits quite well the test results reported in Ref. 10, obtained with a body-flap deflection of 16.15 degrees. This fact points towards the possibility that small geometrical differences between the computed model and the tested one may explain the shift in the calculated value of C_{m0}. At higher angles of attack, the separated vorted wake causes a stabilizing effect and the value of dC_m/dD_L decrease nonlinearly between C_L=0.6 and $C_L\approx$1.0. This phenomenon is predicted by the present method when compared with wind-tunnel data of Ref. 3 (Fig. 5). The experimental data shows, however, a destabilizing effect for C_L>1.0 (possibly due to some viscous phenomenon). This is not predicted in the present calculation.

The variation of the drag coefficient as a function of the angle of attack is presented in Fig. 6. The present method computes only from drag and the induced drag. For comparison with experimental data the calculated results are corrected by adding the value of the experimental C_{D0} so as to obtain the same drag coefficient at zero lift as the experimental value (from Ref. 11). The corrected computed values of C_D are then in good agreement with the experimental data quoted in Ref. 11 and slightly lower than the results obtained using the computational method of Ref. 11.

The canopy effect on the pressure distribution along the upper center-line of the nose section is depicted in Fig. 7. The experimental data as well as the Euler solution are quoted from Ref. 12. The calculation is carried out at α=0 and M=0.6, correcting the incompressible results by the Goethert subsonic similarity rule[13]. The results of the present calculation show a reasonable agreement with the experimental data, considering the coarse axial distribution of the panels used in the nose/canopy region (8-9 panels). It should also be remembered that neither the method of Ref. 12 nor the present method account for viscous effects that may exist in the nose/canopy region. The present results for C_P tend to be higher than the experimental values close to the nose tip, where stagnation of the flow occurs. The calculated values of C_P are slightly lower than the experimental ones over part of the nose upper center line, possibly due to the crude panelling or some slight geometrical inaccuracy in the description of the mode. The pressure rise due to the canopy front end, and also the strong acceleration of the flow around the top of the canopy are well described by the present method.

Figure 8 shows the difference in the pressure coefficient distribution along the upper center line of the nose, between a shuttle configuration that includes a canopy and one that does not include it, at α=0. As expected from the differences in the pressure distributions, the "clean" configuration has a lower form drag and a slightly higher lift coefficient.

The effect of removing the OMS pods at the rear of the shuttle model is shown in Fig. 9. The pressure coefficient is calculated along a longitudinal line passing through the middle of the pod. The presence of the pod affects the pressure distribution well upstream of it. Removal of the OMS pods reduces the form drag of the configuration as expected. Note that these results are obtained even though the OMS pods are very crudely represented by 6 panels circumferentially and only 3 panels longitudinally.

A typical example of the calculated pressure distribution on the wing upper and lower surfaces is presented in Fig. 10 at incidence of 20 deg and axial location of $0.784L_B$. There is a suction peak (the inner one) on the upper surface of the wing due to the vortices emerging from the high sweep portion of the wing that acts similar to a strake. There is also an outer suction peak due to the acceleration of the flow around the blunt leading-edge of the wing in the 45 deg sweep portion, with separated vortices contributing some effect in this region as well. The effect of these vortices is found to be quite small due to the mild sweep and the bluntness of the leading-edge.

Conclusions

The Nonlinear Vortex Lattice method developed originally for slender bodies with arbitrary cross-sections has been applied successfully to the complex geometry of shuttle-like configurations in subsonic flow. The present method predicted correctly the influence of the separated leading-edge vortex flow on the aerodynamic coefficients. Fine details, such as the local effect of a canopy or OMS pods on the pressure distribution, are within the prediction capability of the method. The ability to separate and roll up vortex filaments as a model for the vortex wake makes the present method advantageous over older, linear panel methods that were used for preliminary estimations of NASA space shuttle models[3,14].

The large amounts of data which is generated during the processing of the output of a complex configuration, which is divided into many panels, stresses the need for a graphical visualization that can represent using color coding for pressure distribution for example, and other 3-D graphical methods of representing the computer results.

References

1. Surber, T.E. and Olsen, D.C., "Space Shuttle Orbiter Aerodynamic Development", J. Spacecraft, Vol. 15, No. 1, Jan.-Feb. 1978, pp. 40-47.

2. Bornemann, W.E. and Surber, T.E., "Aerodynamic Design of the Space Shuttle Orbiter", in AGARD CP-247 (High Angle of Attack Aerodynamics), Paper 11, Oct. 1978.

3. Young, J.C. Underwood, J.M., et al., "The Aerodynamic Challenges of the Design and Development of the Space Shuttle Orbiter", NASA CP-2342 (Space Shuttle Technical Conference), Vol. 1, June 1983, pp. 209-263.

4. Hooks, I., Homan, D. and Romere, P., "Aerodynamic Challenges of ALT", NASA CP-2342 (Space Shuttle Technical Conference), Vol. 1, June 1983, pp. 295-312.

5. Rom, J., Almosnino, D. and Gordon, R., "High Angle of Attack Subsonic Non-Linear Vortex Flow Calculations", AIAA Paper 87-2275, AIAA 5th Applied Aerodynamics Conference Proceedings, Aug. 1987, pp. 74-82.

6. Almosnino, D. and Rom, J., "Calculations of Symmetric Vortex Separation Affecting Subsonic Bodies at High Incidence", AIAA J., Vol. 21, No. 3, Mar. 1983, pp. 398-406.

7. Almosnino, D., "High Angle-of-Attack Calculations of the Subsonic Vortex Flow on Slender Bodies", AIAA J., Vol. 23, No. 8, Aug. 1985, pp. 1150-1156.

8. Marconi, F. and Yaeger, L., "Development of a Computer Code for Calculating the Steady Super/ Hypersonic Inviscid Flow Around Real Configurations", NASA CR-2676, Vol. 2, (Code Description), May 1976.

9. Cooke, D.R., "Subsonic Stability and Control Flight Test Results of the Space Shuttle (Tail Cone Off)", AIAA Atmospheric Flight Mechanics Conference Proceedings, CP-806, Aug. 1980, pp. 412-421.

10. Scallion, W.I., et al., "Study of Several Factors Affecting Crew Escape Trajectories from the Space Shuttle Orbiter at Low-Subsonic Speeds", NASA TM-86303, 1985.

11. Harloff, G.J., "High Angle of Attack Hypersonic Aerodynamics", AIAA Paper 87-2548, AIAA 5th Applied Aerodynamics Conference Proceedings, Aug. 1987, pp. 497-505.

12. Szema, K.Y., Chakravarthy, S.R., Pan, D. and Bihari, B.L., "The Application of a Unified Marching Technique for Flow over Complex 3-Dimensional Configurations Across the Mach Number Range", AIAA Paper 88-0276, (AIAA 26th Aerospace Sciences Meeting), Jan. 1988.

13. Brune, G.W. and Rubbert, P.E., "Boundary-Value Problem of Configurations with Compressible Free Vortex Flow", AIAA J., Vol. 15, No. 10, Oct. 1977, pp. 1521-1523.

14. Da Costa, L.A., "Application of Computational Aerodynamics Methods to the Design and Analysis of Transport Aircraft", ICAS Proceedings, Vol. 1, Sept. 1978, pp. 261-269.

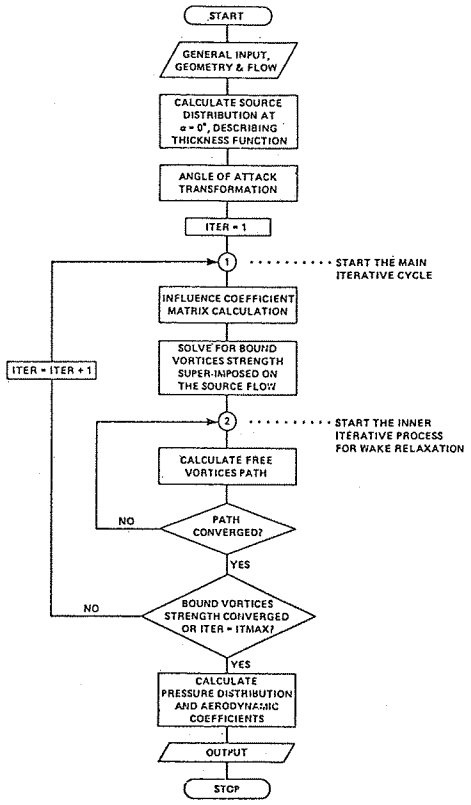

Fig. 1. Flow chart of the non-linear vortex lattice method.

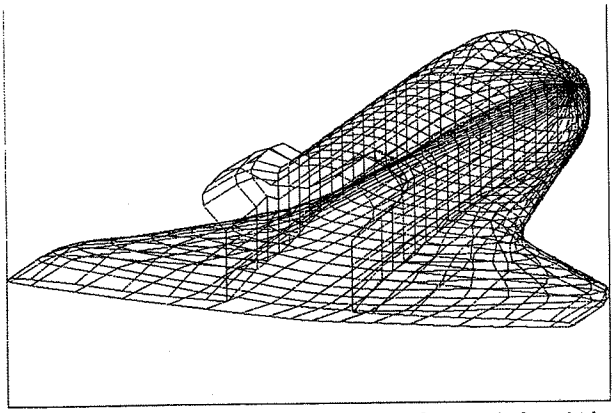

Fig. 2. View of the shuttle model with panel divisions.

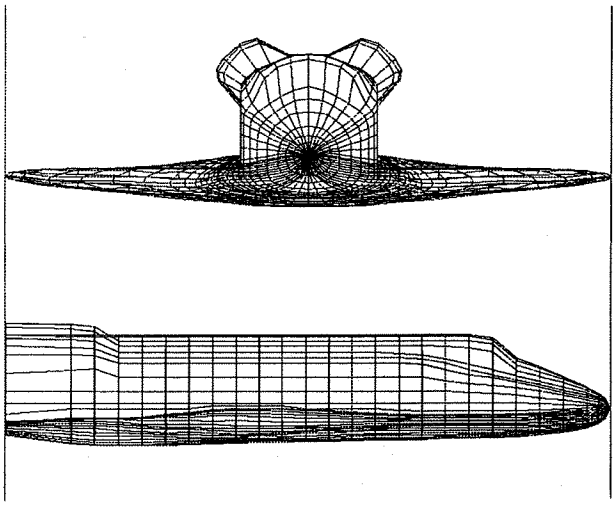

Fig. 3. Front and side views of the panels on the shuttle computer model, including the canopy and pods.

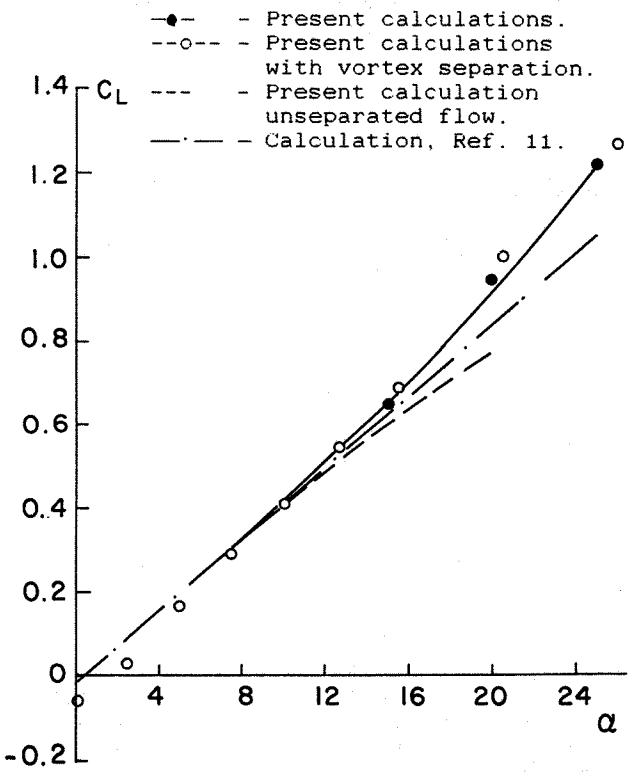

Fig. 4. Variation of the lift coefficient as a function of angle of attack at subsonic speeds.

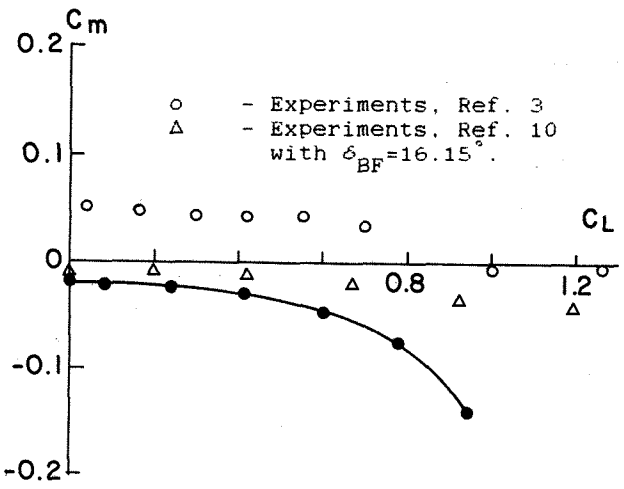

Fig. 5. Variation of the pitching moment coefficient as a function of the Lift coefficient at subsonic speeds.

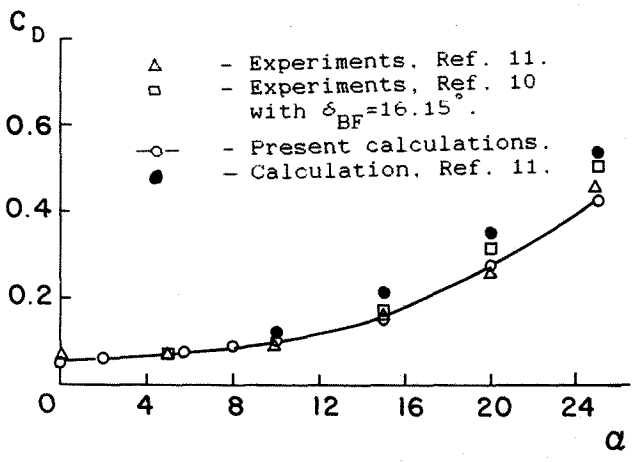

Fig. 6. Variation of drag coefficient as a function of angle of attack at subsonic speeds.

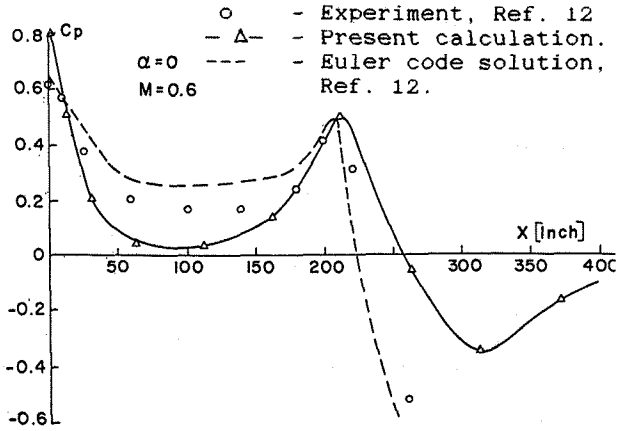

Fig. 7. Pressure distribution on upper center-line of the shuttle hose and canopy.

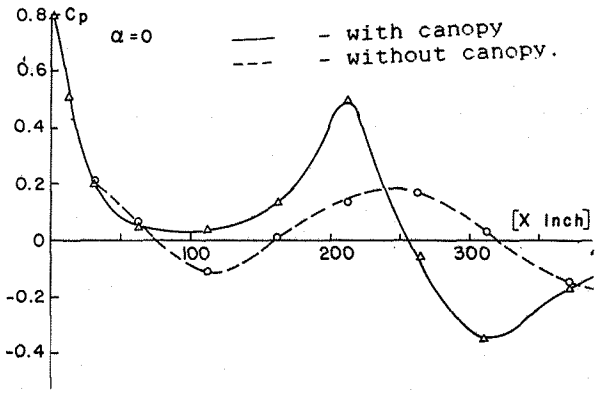

Fig. 8. The effect of the canopy on the pressure distribution.

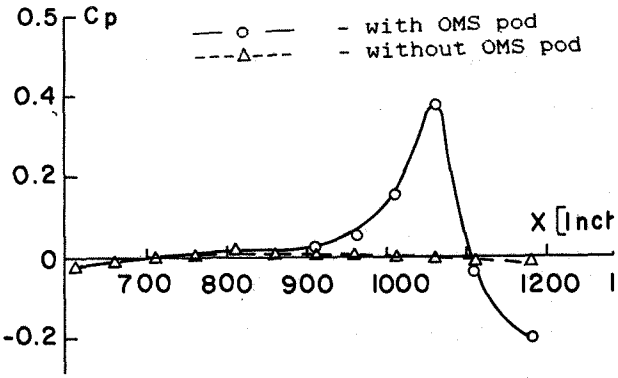

Fig. 9. Effect of OMS pod on pressure distribution (along the OMS pod center line).

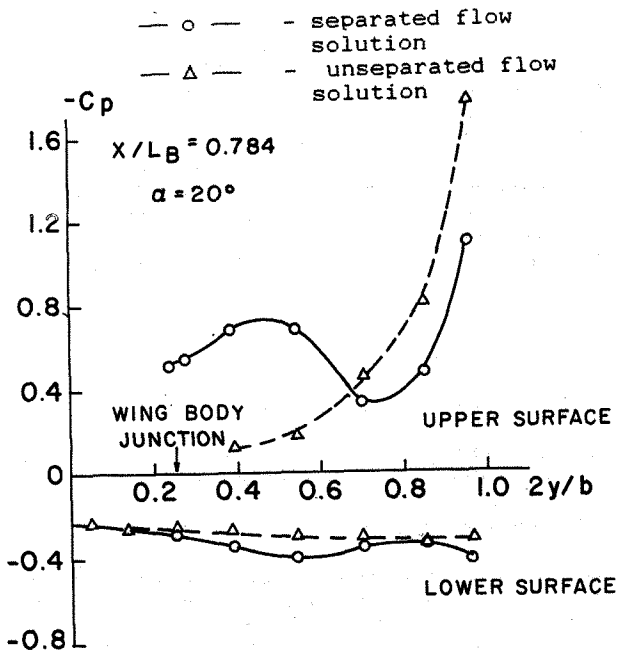

Fig. 10. Pressure distribution on the shuttle wing at $x/L_B=0.784$ and $\alpha=20^{\circ}$.